Pharmaceutical Research, Vol. 24, No. 5, May 2007 (© 2007)
DOI: 10.1007/s11095-006-9204-1

Research Paper

Crystallization Kinetics of Amorphous Griseofulvin by Pattern Fitting Procedure Using X-Ray Diffraction Data

Shigeo Yamamura,[1,2] Rieko Takahira,[1] and Yasunori Momose[1]

Received August 17, 2006; accepted December 4, 2006; published online March 20, 2007

Purpose. A pattern fitting procedure using X-ray powder diffraction patterns was applied to study the crystallization kinetics of amorphous griseofulvin. From the optimized parameters obtained by pattern fitting, a change in the quantity and quality of griseofulvin crystals with crystallization was also investigated.

Materials and Methods. Amorphous griseofulvin was prepared by cooling the melts followed by pulverization. X-ray diffraction patterns of amorphous griseofulvin were repeatedly measured every 20 h. The observed pattern was separated into crystalline diffraction intensity and amorphous scattering intensity by the nonlinear least-squares procedure.

Results. The fitting between the observed and simulated diffraction patterns was satisfactorily independent of the degree of crystallinity. Since a good linear relationship was found in a plot of amorphous scattering intensity against crystalline diffraction intensity, the degree of crystallinity can be determined according to Hermans' method. The diffraction peak width increased with higher diffraction angles with crystallization. The crystallization was biphasic: fast and slow crystallization with the growth of low disordered crystals and disordered crystals, respectively.

Conclusion. The pattern fitting procedure is a powerful tool to analyze the X-ray diffraction patterns of semicrystalline materials. This procedure can simultaneously analyze the degree of crystallinity and crystal disorder in semicrystalline samples during crystallization.

KEY WORDS: crystallinity; crystallization; pattern fitting; powder X-ray diffraction.

INTRODUCTION

The amorphous state is feasible for improving the dissolution rate and bioavailability of poorly water soluble drugs. However, because the physico-chemical stability of an amorphous drug is lower than that of a crystalline one, the crystallization of amorphous drugs would be of concern, particularly when amorphous drugs are used in solid dosage forms.

The crystallization kinetics of amorphous drugs has been studied by X-ray diffraction and thermal analysis (1–3). In the X-ray diffraction method, the amount of the crystalline or amorphous phase in the sample can be determined by quantitative phase analysis using crystalline diffraction intensity and amorphous scattering intensity. Surana *et al.* have conducted studies on the crystallization kinetics of amorphous sucrose based on the increase in integrated intensity of particular diffraction lines (4). Several reports on the quantitative analysis of the crystalline phase or amorphous phase using X-ray methods have been reported (5–7). In these reports, the amount of the crystalline phase was determined from the change in crystalline diffraction intensities of particular diffraction lines.

Because almost all drugs are organic compounds, their crystalline powder would easily show a preferred orientation when packed in a sample plate for X-ray measurement (8). The preferred orientation of crystallites in a sample would lead to the modification of diffraction intensities, and this produces some errors in the quantitative phase analysis by X-ray diffraction methods. Therefore, a correction for the preferred orientation of crystallites would be essential for the quantitative phase analysis by X-ray powder diffraction measurements. There are, however, few reports on the quantitative phase analysis taking into account the preferred orientation of crystallites in a sample.

Furthermore, not only the quantity (degree of crystallinity) but also the quality (lattice disorders) of crystals in semicrystalline samples would affect the pharmaceutical properties of drugs. However, there have been few reports on the quantitative phase analysis taking into account the change in the quality of crystals during crystallization.

In previous reports, we described a pattern fitting procedure for characterizing orthorhombic and monoclinic crystals using powder X-ray diffraction data (9,10). This method is based on the Rietveld analysis in which the effect of the preferred orientation of crystallites on diffraction intensity can be corrected using an appropriate preferred orientation function and the lattice disorder in crystals can be evaluated by peak width parameters (11,12). The Rietveld method is basically a method for crystal structure analysis

[1] School of Pharmaceutical Sciences, Toho University, Miyama 2-2-1, Funabashi, Chiba, 274-8510, Japan.
[2] To whom correspondence should be addressed (e-mail: yamamura@phar.toho-u.ac.jp

Table I. Crystal Structure of Griseofulvin

Formula	$C_{17}H_{17}ClO_6$
Formula weight	352.77
Crystal system	Tetragonal
Space group	P41
a (Å)	8.9721 (8)
c (Å)	19.884 (4)
V (Å^3)	1,600.6 (5)
Z	4
Flack Parameter	−0.03(5)
Number of reflections	9,884
R; Rw	0.066; 0.107
R1	0.036
Goodness-of-fit	1.01

using powder diffraction data, and it has also been applied to the various fields of crystal sciences (13,14). In the future, the pattern fitting procedure can be used to obtain many characteristics of crystals simultaneously, such as the lattice disorder of crystals, preferred orientation of crystallites, lattice constants, etc. (12).

In this study, we applied the pattern fitting procedure to study the crystallization kinetics of amorphous griseofulvin. The X-ray powder diffraction patterns observed during crystallization were divided into crystalline diffraction intensity and amorphous scattering intensity. From the change in the ratio of crystalline and amorphous intensities, the degree of crystallinity was determined by Hermans' method; the crystallization kinetics of amorphous griseofulvin was then investigated. Furthermore, as the crystallization proceeded, the lattice disorder in the crystals was investigated from the scattering angle dependence of the peak width broadening. The purpose of this report is to simultaneously analyze the quantity (degree of crystallinity) and quality (lattice disorder) of the crystals during the crystallization of amorphous griseofulvin by the pattern fitting procedure.

MATERIALS AND METHODS

Materials

Griseofulvin was of the reagent grade (Sigma Chemical Co., St. Louis, MO., USA). A single crystal of griseofulvin for crystal structure analysis was obtained by crystallization from an ethanol solution at room temperature. Crystalline griseofulvin powder was prepared by passing the crystallized griseofulvin through a 250 mesh (63 μm) sieve. Amorphous griseofulvin was prepared by cooling the melt. After amorphous griseofulvin was pulverized by a mortar and pestle, the powder was passed through a 250 mesh (63 μm) sieve. The amorphous griseofulvin powder was packed in an aluminum sample plate immediately after its preparation.

Crystal Structure Analysis

The crystal structure of griseofulvin was determined by the RASA system (Rigaku, Tokyo, Japan). The X-ray source was Mo-Kα radiation with a voltage of 50 kV and a current of 200 mA. Diffraction data were collected at 298 K. The

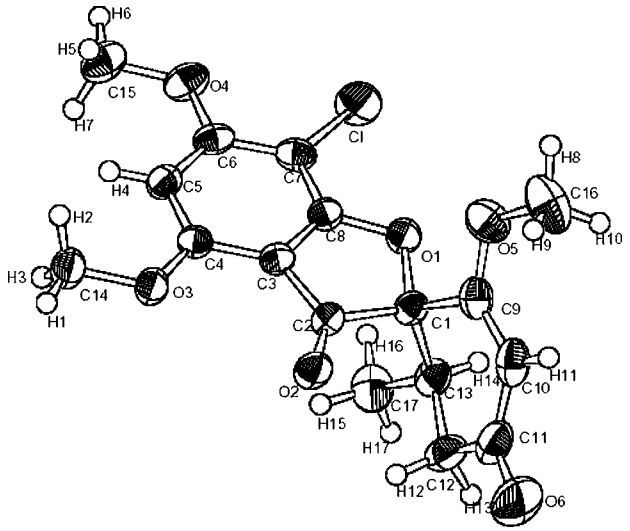

Fig. 1. Oak ridge thermal ellipsoid plot (ORTEP) of griseofulvin molecules.

structure was solved by a direct method and refined using full-matrix least squares method on the basis of F_0^2 . Non-hydrogen atoms were anisotropically refined, and the absolute structure of griseofulvin was determined by using the Flack parameter. A summary of the crystal structure analysis is given in Table I, and the structure is shown as an oak ridge thermal ellipsoid plot (ORTEP) diagram in Fig. 1. The crystal structure factors used in the pattern fitting were calculated from the refined crystal structure of griseofulvin.

The crystal structure of griseofulvin has already reported (15). However, since limited information on the crystal structure is given in literatures, we had to determine the crystal structure of griseofulvin in our study.

Powder X-ray Diffraction

The powder X-ray diffraction intensities were measured using a RINT 2500 X-ray diffractometer (Rigaku Co., Tokyo, Japan), and symmetrical reflection geometry was employed. The X-ray source was Cu-Kα radiation with a voltage of 50 kV and a current of 100 mA. The diffracted X-ray beam was monochromated by a bent graphite monochromator, and a scintillation counter was used as the detector. Diffraction

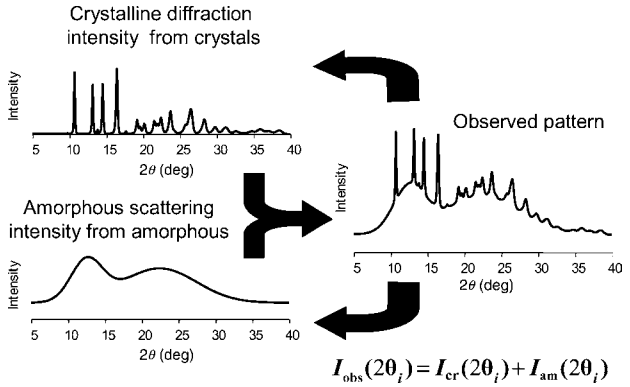

Fig. 2. Basic concept of pattern-fitting to separate into crystalline diffraction intensity and amorphous scattering intensity.

intensities were measured by a fixed-time step-scanning method in the range of 5–40° (2θ) at an interval of 0.02°. The measurement was carried out at room temperature and repeated every 20 h. The X-ray absorption by the specimen and the contribution of Cu-Kα_2 to the observed diffraction intensity were ignored in the pattern fitting calculation.

Pattern-fitting

A computer program for pattern fitting was developed using the MATLAB software version 6.12 with optimization and statistics toolboxes (The Math Works Inc., MA., USA). The trust-region reflective Newton method was applied to optimize the fitting parameters (16,17).

RESULTS

Theoretical Background of Pattern Fitting

The observed X-ray diffraction pattern was assumed to consist of discrete diffraction intensities from the crystalline phase (crystalline diffraction intensity) and halo intensities from the amorphous phase (amorphous scattering intensity).

The crystalline diffraction intensity was simulated by the X-ray diffraction theory using the information of the crystal structure as given by Eq. 1 (11,18).

$$I(2\theta_i) = K_{cr}\sum_n F_{hkl}^2 \cdot m_{hkl} \cdot Lp_{hkl} \cdot G(2\theta_{hkl} - 2\theta_i) \cdot P_{hkl} \quad (1)$$

where $I(2\theta_i)$ is the observed crystalline diffraction intensity at $2\theta_i$; K_{cr}, the normalization constant; n, the number of *hkl* reflections; F_{hkl}, the crystal structure factor of the nth *hkl* reflection; m, the multiplicity factor; Lp, the Lorentz-polarization factor; and $2\theta_{hkl}$, the scattering angle of an *hkl* reflection calculated from the lattice constants and the Miller indices of the *hkl* reflection, as expressed by Eq. 2.

$$\theta = \sin^{-1}\left\{\frac{\lambda}{2}\sqrt{\frac{h^2+k^2}{a^2}+\frac{l^2}{c^2}}\right\} \quad (2)$$

where a and c are the lattice constants of the tetragonal griseofulvin crystal.

G is the profile function (we used the modified Lorentz function (19)) as represented by Eq. 3; H is the full width at half maximum (FWHM), Eq. 4; and s is the asymmetric parameter, Eq. 5.

$$G = 2sc_{ML}^{0.5}\Big/\left\{\pi H\left(1+c_{ML}(2\theta_{hkl}-2\theta_i)^2\Big/H^2\right)^2\right\} \quad (3)$$

$$H^2 = U\tan^2\theta_{hkl} + V\tan\theta_{hkl} + W \quad (4)$$

$$s = 1 - A\cdot\mathrm{sign}(2\theta_{hkl}-2\theta_i)(2\theta_{hkl}-2\theta_i)^2\Big/\tan\theta_{hkl} \quad (5)$$

where s is the function for the correction of the peak asymmetry and c_{ML} is the normalization constant for the modified Lorentz function (19). U, V, and W in Eq. 4 are the peak width parameters (18), and A in Eq. 5 is the asymmetric parameter.

Table II. Reflecting Plane Indices, Structure Factors, and Multiplicity Factors used in Pattern Fitting

h	k	l	F	m	h	K	l	F	m	h	k	l	F	m
1	0	0	5.3	4	2	2	0	32.9	4	1	1	7	20.1	8
1	0	1	51.3	8	2	2	1	2.6	8	3	0	4	40.3	8
1	0	2	61.6	8	2	1	4	83.1	8	2	1	6	9.7	8
1	1	0	22.5	4	1	2	4	90.2	8	1	2	6	47.4	8
1	1	1	67.8	8	1	0	6	4.5	8	2	3	0	71.6	4
1	1	2	82.4	8	2	2	2	25.4	8	3	2	0	47.8	4
1	0	3	62.0	8	3	0	0	19.1	4	0	0	8	43.3	2
0	0	4	46.5	2	2	0	5	82.3	8	2	2	5	34.2	8
1	1	3	60.5	8	3	0	1	42.4	8	3	2	1	11.0	8
2	0	0	52.8	4	1	1	6	15.7	8	2	3	1	21.2	8
2	0	1	34.7	8	3	0	2	46.9	8	1	3	4	45.9	8
1	0	4	49.7	8	2	2	3	28.5	8	3	1	4	47.5	8
2	0	2	65.6	8	3	1	0	24.7	4	2	3	2	7.5	8
2	1	0	27.3	4	1	3	0	84.3	4	3	2	2	55.3	8
1	2	0	65.3	4	2	1	5	32.7	8	2	0	7	33.1	8
1	2	1	51.3	8	1	2	5	38.5	8	1	0	8	56.3	8
2	1	1	37.4	8	1	3	1	34.2	8	3	0	5	18.5	8
1	1	4	59.4	8	3	1	1	5.7	8	2	3	3	35.5	8
1	2	2	42.9	8	3	1	2	25.7	8	3	2	3	41.0	8
2	1	2	22.0	8	1	3	2	25.0	8	2	1	7	11.0	8
2	0	3	100.7	8	3	0	3	39.0	8	1	2	7	38.1	8
1	0	5	40.9	8	1	0	7	43.3	8	1	1	8	75.3	8
2	1	3	39.8	8	2	2	4	26.1	8	3	1	5	26.4	8
1	2	3	51.0	8	2	0	6	23.6	8	1	3	5	30.0	8
1	1	5	75.7	8	1	3	3	16.9	8	2	2	6	28.0	8
2	0	4	139.6	8	3	1	3	4.2	8					

P in Eq. 1 is the preferred orientation function as follows

$$P_{hkl} = \exp\left(-\alpha\varphi_{hkl}^2\right) \tag{6}$$

where α is the preferred orientation parameter indicating the strength of the preferred orientation of the crystallites in the sample, and φ is the acute angle between the preferred orientation plane (normal to the preferred orientation axis) and the (*hkl*) plane. The preferred orientation plane was selected to be the (001) plane because the best fit was then achieved by a trial and error approach.

The amorphous scattering intensity in the observed X-ray pattern was postulated to be proportional to the halo scattering intensity of amorphous griseofulvin before crystallization.

Finally, the observed X-ray diffraction patterns of semicrystalline samples were expressed as follows:

$$I_{\text{obs}}(2\theta_i) = K_{cr}\sum_n F_{hkl}^2 \cdot m_{hkl} \cdot Lp_{hkl} \cdot G(2\theta_{hkl} - 2\theta_i) \cdot P_{hkl} + K_{\text{am}} I_{\text{am}}(2\theta_i) \tag{7}$$

where K_{am} is the proportional constant of the observed amorphous scattering intensity to the halo scattering intensity of amorphous griseofulvin (I_{am}).

In the process of pattern fitting, the crystal lattice parameters (a and c), FWHM parameters (U, V, and W), asymmetric parameter (A), preferred orientation parameter (α), and normalization constants (K_{cr} and K_{am}) were optimized simultaneously in order to minimize the sum (Eq. 8) using the nonlinear least squares procedure.

$$\text{Sum} = \sum_{i=1}^{N}\left(w_i(I_{obs}(2\theta_i) - I_{cal}(2\theta_i))^2\right) \tag{8}$$

where N is the number of data points, w_i is the weight of the data ($1/I_{\text{obs}}(2\theta_i)$), and $I_{\text{obs}}(2\theta_i)$ and $I_{\text{cal}}(2\theta_i)$ are the observed and calculated intensities at $2\theta_i$, respectively.

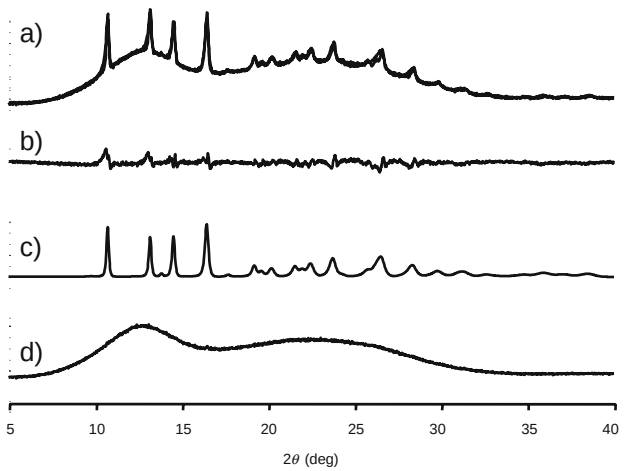

Fig. 3. Typical example of separation of crystalline diffraction intensity and amorphous scattering intensity by pattern fitting **a** original intensity, **b** difference between original and simulated intensities, **c** crystalline diffraction intensity, **d** amorphous scattering intensity.

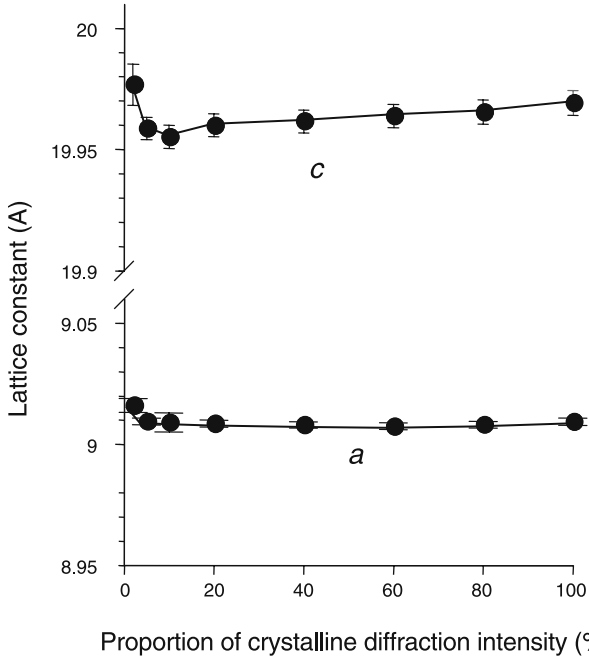

Fig. 4. Plot of optimized parameter of crystal lattice constants with proportion of crystalline diffraction intensity in test patterns.

After the observed intensities are fit into Eq. 7, the observed pattern can be decomposed into the crystalline diffraction intensity and the amorphous scattering intensity. From the separated crystalline diffraction intensity, several crystallographic parameters of the griseofulvin crystals in the samples can be simultaneously obtained from the optimized parameters. The concept of pattern fitting to

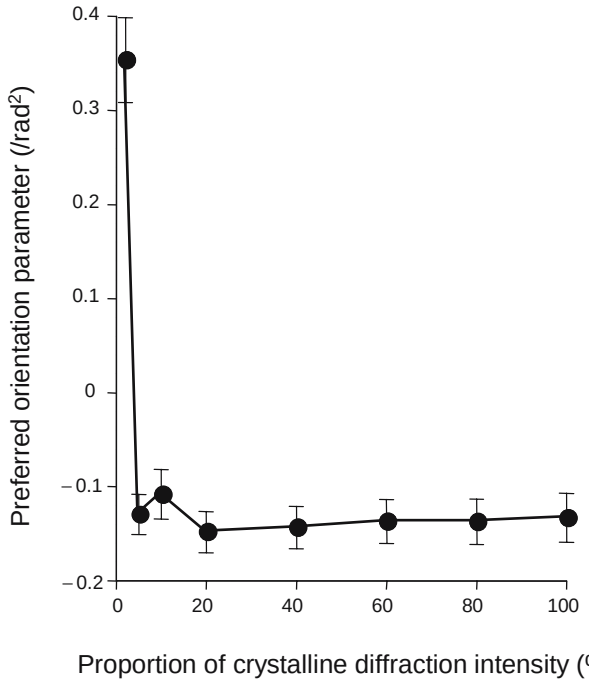

Fig. 5. Plot of optimized parameter of preferred orientation parameter with proportion of crystalline diffraction intensity in test patterns.

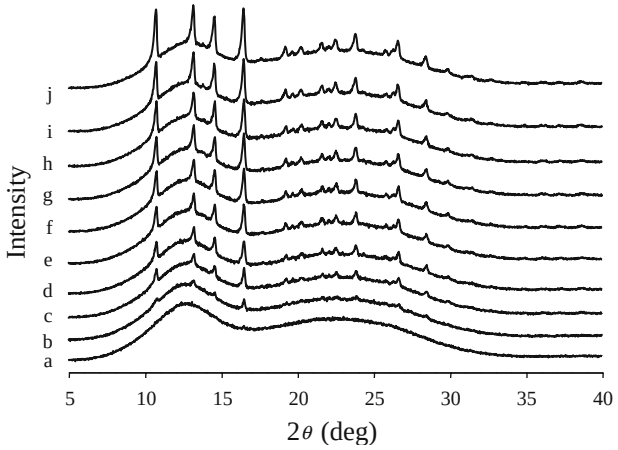

Fig. 6. Change in the X-ray diffraction pattern of amorphous griseofulvin with crystallization **a** amorphous griseofulvin, **b** 40 h, **c** 80 h, **d** 120 h, **e** 160 h, **f** 200 h, **g** 240 h, **h** 280 h, **i** 480 h, **j** 880 h.

decompose into crystalline intensity and amorphous intensity is illustrated in Fig. 2.

The diffraction plane indices, crystal structure factors, and multiplicity of the griseofulvin crystal used in the pattern fitting are summarized in Table II. The intensity data of all the reflections observed theoretically between 5–40° (2θ) were used in the pattern fitting calculation. Figure 3 shows a typical example of the decomposition into crystalline diffraction intensity and amorphous scattering intensity by pattern fitting.

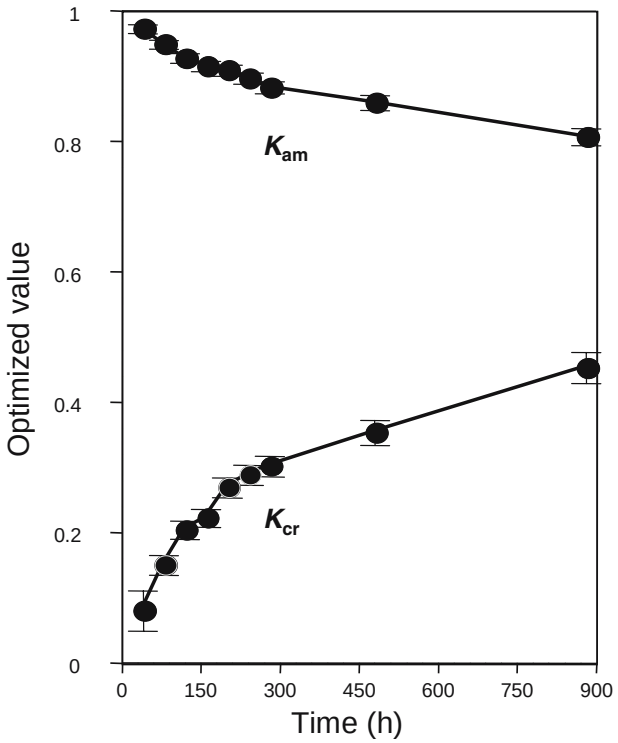

Fig. 7. Change in K_{cr} and K_{am} with crystallization of amorphous griseofulvin Bars represent 95% CI of estimated values.

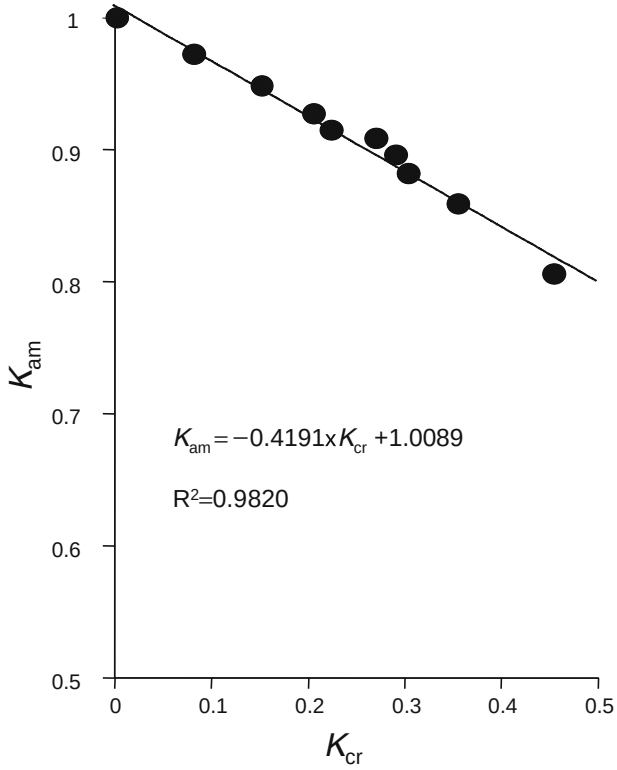

Fig. 8. Plot of K_{am} against K_{cr}.

Lower Limit of Detection of Crystal Contents by Pattern Fitting

The lower limit of the detection of griseofulvin crystal content by the pattern fitting procedure was investigated as follows: the test diffraction patterns were generated with variable proportions of crystalline diffraction intensity measured with the crystalline griseofulvin powder and amor-

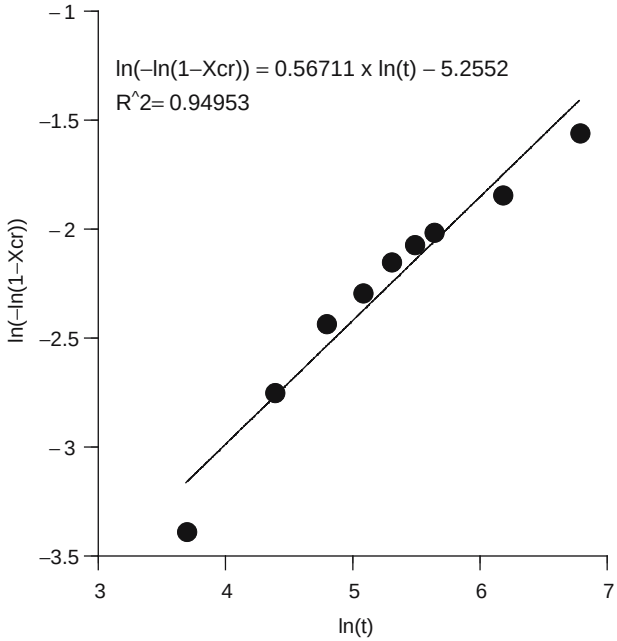

Fig. 9. Plot of ln(-ln(1-X_{cr})) *vs* ln *t* for crystallization of amorphous griseofulvin.

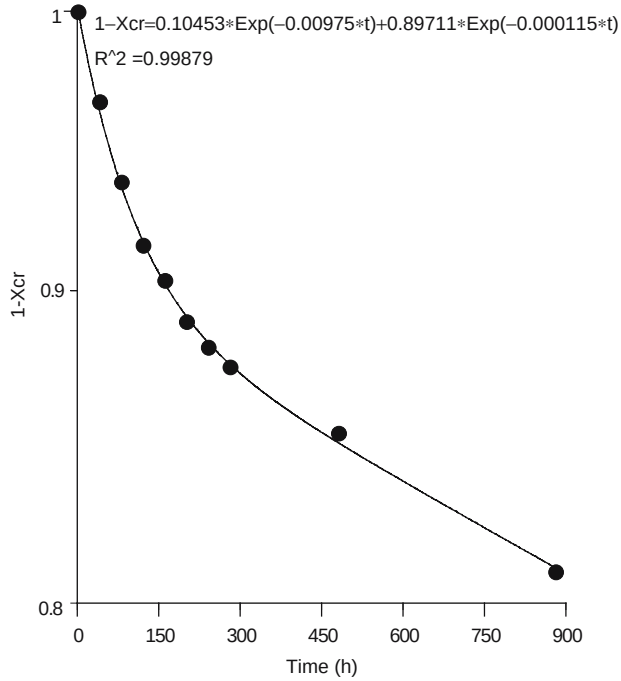

Fig. 10. Plot of $\ln(1\text{-}X_{cr})$ *vs* *t* for crystallization of amorphous griseofulvin.

phous halo intensity measured with the amorphous griseofulvin powder. The lower limit of crystal contents to reproduce the original crystallographic parameters was determined from the optimized parameters by pattern fitting using test patterns.

Figures 4 and 5 indicate the plot of the lattice constants and the preferred orientation parameters with the proportion of crystalline diffraction intensity. The marks at 100% crystalline diffraction intensity indicate the parameters obtained by pattern fitting with the crystalline griseofulvin powder. The ratio of the crystalline and amorphous intensities of the optimized parameters obtained using the test patterns was 2.5:97.5; these parameters had a large standard error of estimation and were not considered to indicate the characteristics of the crystals in the sample. When using the test patterns with a crystalline diffraction intensity of more than 5%, the confidence intervals of the optimized parameters overlapped with each other and also with those obtained with the crystalline griseofulvin powder. These results indicate that when the crystal content in a sample is more than about 5%, the optimized parameters by pattern fitting are considered to indicate the characteristics of the griseofulvin crystals in the sample. Therefore, the lower limit of the crystal content in the sample was determined to be about 5% by pattern fitting.

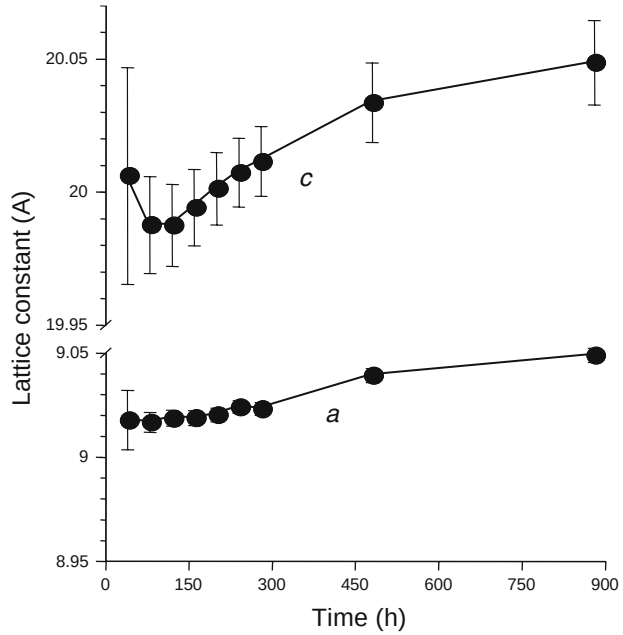

Fig. 11. Change in the crystal lattice constants of griseofulvin with crystallization of amorphous griseofulvin Bars represent 95% CI of estimated values.

Change in Characteristics of Griseofulvin Crystals During Crystallization

Figure 6 shows the change in the X-ray diffraction patterns of amorphous griseofulvin on standing. There were no diffraction peaks in the pattern measured at 0 h. The crystalline diffraction intensity was then found in the pattern measured after standing for 40 h and it increased as time elapsed, indicating that crystallization occurred gradually. The observed diffraction patterns after standing for 40 h or longer were used for the pattern fitting. All the fittings between the observed and simulation patterns were satisfactory, as shown in Fig. 3. By pattern fitting, accompanied with the decomposition of crystalline diffraction intensity and amorphous scattering intensity, some crystallographic parameters of the griseofulvin crystals in the sample can also be optimized simultaneously. From the change in the optimized parameters, the characteristics of the griseofulvin crystals during crystallization were investigated.

Figure 7 shows the change in optimized K_{cr} and K_{am} with the crystallization of amorphous griseofulvin. As crystallization proceeded, K_{am} decreased while K_{cr} increased. K_{cr}

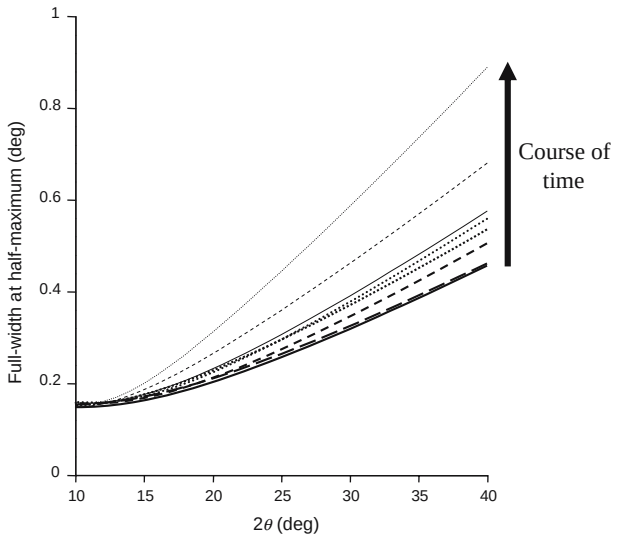

Fig. 12. Change in the FWHM of griseofulvin with crystallization of amorphous griseofulvin 40 h, 80 h, 120 h, 160 h, 200 h, 280 h, 480 h, 880 h.

and K_{am} are considered to be the indicators of crystalline diffraction intensity and amorphous scattering intensity, respectively. If a plot of K_{am} against K_{cr} would show a linear relationship, the degree of crystallinity can be determined by Hermans' method (20). Since a good linear relationship was found, as shown in Fig. 8, the degree of crystallinity of each sample can be determined by Hermans' method.

Figures 9 and 10 show the change in the crystallinity of griseofulvin during crystallization plotting with Eqs. 9 and 10.

$$\ln(-\ln(1 - X_{CR})) = \alpha \cdot \ln(t) + b \tag{9}$$

$$(1 - X_{CR}) = \alpha_1 \exp(-b_1 \cdot t) + \alpha_2 \exp(-b_2 t) \tag{10}$$

Equation 9 is a logarithmic form of the Avrami-Erofeev equation. (21,22). This model considers crystallization process with nucleation and growth. If a plot of ln(−ln(1-Xcr)) against t shows a linear relationship, a slope, a, represents the dimensional order of the nucleation and crystal growth process. As shown in Fig. 9, the plot did not give a good straight line. This result suggests that the crystallization of amorphous griseofulvin did not follow simple nucleation and growth model. On the other hand, a plot with Eq. 10 showed good fit between observed and calculated values. This result indicates that the crystallization process of amorphous griseofulvin was biphasic: a fast crystallization process at the early stage of crystallization and then a slow crystallization process at a later stage.

Figure 11 shows the change in the lattice constants of the griseofulvin crystals determined by pattern fitting during crystallization. At an initial stage of crystallization, the optimized lattice constants had a large standard error of estimation. This is because a minor part of the sample had crystallized and the crystalline diffraction intensity was extremely weak. As crystallization proceeded, the lattice constants gradually increased while the standard error of estimation decreased.

Figure 12 shows the change in the FWHM of the diffraction peaks with the scattering angle as crystallization proceeded, calculated from the optimized U, V, and W values obtained by pattern fitting. The diffraction peaks were not observed to broaden at lower scattering angles, and a marked increase in the broadening was found at higher scattering angles with crystallization.

DISCUSSION

The fitting between the observed diffraction patterns and simulation patterns were satisfactory, and the fitting parameters were significantly optimized (the 95% confidence intervals of the estimates of all the fitting parameters did not include 0). From the fitting results, the degree of crystallinity was calculated and the crystallization process of amorphous griseofulvin was found to be biphasic: a fast crystallization process at the early stage of crystallization and then a slow crystallization process at a later stage.

A broadening of the diffraction peak is affected by both the crystallite size and the lattice disorder (23). In the paracrystal theory, the broadening of diffraction peaks is attributed to crystallites smaller than 1,000 Å. The broadening is independent of the scattering angle. Also, the lattice disorder results in an increase in the peak width with the scattering angle (24). The marked increase in the peak width at higher angles with crystallization is attributed to the growth of disordered crystals at a later stage of crystallization.

It was found that the lattice constants increased and the FWHM of the peaks at higher diffraction angles markedly increased with crystallization; these results indicate that the disordered griseofulvin crystals were grown at a later stage of crystallization.

As a whole, the crystallization process of amorphous griseofulvin was considered to be as follows: at the first stage of crystallization, griseofulvin crystals with a slight lattice disorder were formed and the disordered griseofulvin crystals were then grown as crystallization proceeded.

In conclusion, the pattern fitting procedure is a powerful tool to trace the crystallization kinetics of amorphous samples. In pattern fitting, the degree of crystallinity and the characteristics of the crystals in semicrystalline samples were determined simultaneously. The crystallization of amorphous griseofulvin was found to be biphasic: fast crystallization with the growth of low disordered crystals and slow crystallization with the growth of disordered crystals.

REFERENCES

1. C. Nunes, A. Mahendrasingam, and R. Suryanarayanan. Quantification of crystallinity in substantially amorphous materials by synchrotron X-ray powder diffractometry. *Pharm. Res.* **22**:1942–1953 (2005).
2. S. J. Byard, S. L. Jackson, A. Smail, M. Bauer, and D. C Apperley. Studies on the crystallinity of a pharmaceutical development drug substance. *J. Pharm. Sci.* **94**:1321–1335 (2005).
3. M. K. Haque and Y. H. Roos. Crystallization and X-ray diffraction of spray-dried and freeze-dried amorphous lactose. *Carbohydr. Res.* **340**:293–301 (2005).
4. R. Surena and R. Suryanarayanan. Quantitattion of crystallinity in substantially amorphous pharmaceuticals and study of crystallization kinetics by X-ray powder diffractometry. *Powder Diff.* **15**:2–6 (2000).
5. M. Otsuka, F. Kato, Y. Matsuda, and Y. Ozaki. Comparative determination of polymorphs of indomethacin in powders and tablets by chemometrical near-infrared spectroscopy and X-ray powder diffractometry. *AAPS Pharm. Sci. Tech.* **4**:147–158 (2003).
6. I. Fix and K. J. Steffens. Quantifying low amorphous or crystalline amounts of alpha-lactose-monohydrate using X-ray powder diffraction, near-infrared spectroscopy, and differential scanning calorimetry. *Drug Dev. Ind. Pharm.* **30**:513–523 (2004).
7. P. Bergese, I. Colombo, D. Gervasoni, and L. E. Depero. Assessment of the X-ray diffraction-absorption method for quantitative analysis of largely amorphous pharmaceutical composites. *J. Appl. Crystallogr.* **36**:74–79 (2003).
8. S. N. C. Roberts, A. C. Williams, I. M. Grimsey, and S. W. Booth. Quantitative analysis of mannitol polymorphs. X-ray powder diffractometry-exploring preferred orientation effects. *J. Pharm. Biomed. Anal.* **28**:1149–1159 (2002).
9. S. Yamamura and Y. Momose. Quantitative analysis of crystalline pharmaceuticals in powders and tablets by a pattern-fitting procedure using X-ray powder diffraction data. *Int. J. Pharm.* **212**:203–212 (1991).
10. S. Yamamura and Y. Momose. Characterization of monoclinic crystals in tablets by pattern-fitting procedure using X-ray powder diffraction data. *Int. J. Pharm.* **259**:27–37 (2003).

11. H. M. Rietveld. A profile refinement method for nuclear and magnetic structure. *J. Appl. Crystallogr.* **2**:65–71 (1969).
12. R. Delhez, T. H. de Keijser, J. I. Langford, D. Louer, E. J. Mittemeijer, and E. J. Sonneveld. Crystal imperfection broadening and peak shape in the Rietveld method. In R. A. Young (ed.)., *The Rietveld Method*, Oxford University Press, New York, 1993, pp. 132–166.
13. B. M. Kariuki, K. Psallidas, K. D. M. Harris, R. L. Johnston, R. W. Lancaster, S. E. Staniforth, and S. M. Cooper. Structure determination of a steroid directly from powder diffraction data. *Chem. Commun. (Cambridge)* **17**:1677–1678 (1999).
14. A. Pratapa, B. O'Connor, and B. Hunter. A comparative study of single-line and Rietveld strain-size evaluation procedures using MgO ceramics. *J. Appl. Crystallogr.* **35**:155–162 (2001).
15. G. Malmos, A. Wagner, and L. Maron. (2S,6′R)-7-chloro-2′,4,6, -trimethoxy-6′-methyl-spiro-(benzofuran-2(3H),2-(2′)cyclohexane) -3,4′-dione $C_{17}H_{17}ClO_6$. *Cryst. Struct.Commun.* **6**:463–470 (1977).
16. T. F. Coleman and Y. Li. On the convergence of reflective Newton methods for large-scale nonlinear minimization subject to bounds. *Math. Programming.* **67**:189–224 (1994).
17. T. F. Coleman and Y. Li. An interior region approach for nonlinear minimization subject to bounds. *SIAM J. Optimization.* **6**:418–445 (1996).
18. R. A. Young. Introduction to the Rietveld method. In R. A. Young (ed.)., *The Rietveld Method*, Oxford University Press, New York, 1993, pp. 1–38.
19. E. J. Sonneveld and J. W. Visser. Automatic collection of powder data from photographs. *J. Appl. Crystallogr.* **8**:1–7 (1975).
20. P. Hermans and A. Weidinger. Quantitative x-ray investigation on the crystallinity of cellulose fibers. A background analysis. *J. Appl. Phys.* **19**:491–506 (1948).
21. C. Michaelsen and M. Dahms. On the determination of nucleation and growth kinetics by calorimetry. *Thermochim. Acta.* **288**:9–27 (1996).
22. H. H. Y. Tong, B. Y. Shekunov, J. P. Chan, C. K. F. Mok, H. C. M. Hung, and A. H. L. Chow. An improved thermoanalytical approach to quantifying trace levels of polymorphic impurities in drug powders. *Int. J. Pharm.* **295**:191–199 (2005).
23. H. P. Klug and L. E. Alexander. *X-ray Diffraction Procedures for Polycrystalline and Amorphous Materials*, 2nd edn. Wiley, New York, 1974, pp. 618–708.
24. R. Hosemann and S. N. Bagchi. *Direct Analysis of Diffraction by Matter*, North Holland, Amsterdam, 1962.